Arabian Journal of Chemistry (2022) **15**, 103477

King Saud University

Arabian Journal of Chemistry

www.ksu.edu.sa
www.sciencedirect.com

ORIGINAL ARTICLE

Design, synthesis and application of a sponge-like nanocomposite ceramic for the treatment of Ni(II) and Co(II) wastewater in the zinc ingot industry

Sayed Asaad Abdollahi, Nader Mokhtariyan *, Elham Ameri

Department of Chemical Engineering, Shahreza Branch, Islamic Azad University, P.O. Box 311-86145 Shahreza, Iran

Received 12 August 2021; accepted 3 October 2021
Available online 11 October 2021

KEYWORDS

Adsorption;
Heavy metal;
Wastewater;
Sponge-like nanocomposite ceramic;
Clay;
Hydroxyapatite

Abstract In this study, a sponge-like nanocomposite ceramic was made of clay, bovine bone nano-powder, and human hair; to remove Ni(II) and Co(II) ions from synthetic and industrial wastewaters. The structure of sponge-like nanocomposite ceramic was investigated with XRD (Hexagonal structural type of hydroxyapatite) and functional groups were identified using FT-IR (Hydroxyl @ 3573 cm^{-1} and Phosphate @ 1045 cm^{-1}). The specific surface and morphology of the ceramic-based on BET (172.46 m^2g^{-1}) and FE-SEM (Nano-hydroxyapatite: 100 nm), respectively showed that the use of human hair creates good porosity. The process was optimized at pH 6, temperature 40 ℃, adsorbent mass 17 g, initial concentration iofns 233 mg L^{-1}, and retention time 178 min. Kinetic models, thermodynamic parameters and, isotherm models were applied to describe the adsorption equilibrium data. The Ni(II) and Co(II) adsorption efficiency, from industrial wastewaters, were more than 95%. The adsorbents could be regenerated and reused for up to 60 consecutive cycles.

1. Introduction

Heavy metals are released into the environment as a result of a variety of industrial activities. Toxic ions can adversely affect the health of all living organisms (Akbarzadeh et al., 2020). Therefore, removing or reducing the concentration of heavy metal ions from the wastewater is an important issue, as the rules of the World Health Organization (WHO) emphasize that industrial effluents must be treated before entering the environment and the level of pollution must be reduced to the specified allowable amount (Cui et al., 2018).

Given the importance of removing heavy metals, researchers around the world are trying to find ways to effectively remove these compounds. The main techniques in this regard include ion exchange, chemical precipitation, membrane filtration, and adsorption or biosorption. Biosorption is less costly because biosorbents are generally made from different waste (Yu et al., 2021); also the operating conditions in this process have a wide range of pH, temperature and concentration, unlike techniques such as adsorption with activated carbon, precipitation, reverse osmosis or dialysis (Hernández-Cocoletzi et al., 2020).

* Corresponding author.
E-mail address: mokhtarian@iaush.ac.ir (N. Mokhtariyan).
Peer review under responsibility of King Saud University.

Production and hosting by Elsevier

https://doi.org/10.1016/j.arabjc.2021.103477
1878-5352

Hydroxyapatite is a biocrystal and main inorganic component of bone with the chemical formula $Ca_{10}(PO_4)_6(OH)_2$ (Guo et al., 2019).

Hydroxyapatite is widely used today. Faksawat et al. (Faksawat et al., 2021) synthesized ceramics from a mixture of hydroxyapatite and natural clay with 3D printing technology for medical applications. Kundu et al. (Kundu et al., 2021) synthesized nanofibers using hydroxyapatite/clay to produce 3D scaffolds for use in tissue engineering. Ebadzadeh et al. (Ebadzadeh et al., 2011) mixed a 10 mm thick layer of clay, hydroxyapatite and alumina, after a pressure of 255 MPa, placed at 1350 ℃ for 2 h, the product was a porous membrane. Various studies show that hydroxyapatite has a high adsorption capacity for the adsorption of heavy metal ions due to its excellent ion exchange property. Hydroxyapatite has buffering properties and also has low solubility in water and has high stability during oxidation. It is effective in the treatment of industrial effluents to remove heavy metal ions such as lead, zinc, nickel, cobalt, copper, cadmium, and lead with an adsorption capacity of 254.90 mgg^{-1} (Zou et al., 2019). Ersan et al. (Ersan et al., 2015) synthesized porous ceramics with clay and hydroxyapatite to adsorb tetracycline from the aqueous medium, this ceramic had a high adsorption capacity. RoyChoudhury et al. (Roychoudhury et al., 2019) used a hydroxyapatite/clay membrane to remove lead ions from industrial wastewater in a pressurized system within a circular modulus. Googerdchian et al. (Googerdchian et al., 2018) examined four effective operational parameters including bovine bone ball milling time, the initial concentration ion, pH, and dosage, in the lead adsorption from aqueous solutions by nanohydroxyapatite, their results at pH 3 showed the highest removal efficiency with maximum sorption capacity of 200 mg g^{-1}. According to dissolution of Hydroxyapatite at low pH value of 3 and formation of hydroxypyromorphite reported the main adsorption mechanism is dissolution-precipitation (Shen et al., 2016). Zeng et al. (Zeng et al., 2019) connected sodium, silicate and carbonate ions to hydroxyapatite with the sonochemistry coprecipitation and built an ion exchange adsorbent for remove lead and cadmium ions; this adsorbent confirmed its stability in four replications of the adsorption and desorption process while maintaining its properties. Hamad et al. (Hamad et al., 2020) to take advantage of the attractive properties of cellulose acetate and hydroxyapatite, used the electrospinning technique to the synthesis of an adsorbent with high stability for the removal of lead and iron.

In addition to organic origin, mineral origin such as natural zeolite, calcium silicate powders and natural clay are used to remove heavy metal ions. Porosity is very important in these adsorbents, as Padilla-Ortega et al. (Padilla-Ortega et al., 2013) reported that the bentonite, sepiolite and vermiculite clays had a specific surface area of 41.7, 194 and 15.2 m^2g^{-1}, respectively and pore volume of 0.063, 0.30 and 0.049 cm^3g^{-1}, respectively. Mouiya et al. (Mouiya et al., 2019) made a ceramic membrane of clay to treat industrial effluent, they used banana peel powder to create porosity. Hubadillah et al. (Hubadillah et al., 2020) synthesized a bioceramic membrane with a hollow fiber structure based on hydroxyapatite and completely removed heavy metal ions from textile effluents; their results showed that by increasing the sintering temperature from 900 to 1200 ℃, the porosity decreases and the highest porosity was obtained at 900 ℃. The adsorbents such as nanohydroxyapatite to remove heavy metal ions is highly effective, but it is difficult to separate these adsorbents from the treated wastewater. Natural clays offer a special low surface area for adsorption, they have a low adsorption kinetics of heavy metal ions, and they are difficult to regenerate (Liu et al., 2021). In conventional adsorption systems, the adsorbents on a micro or nano-meter scale are in contact with the wastewater, and after the adsorption process, filtration must be performed to separate the adsorbent from the Treated wastewater. This sponge-like ceramic is much easier to use and does not require the cost of separating the adsorbent from the treated wastewater fluid. In this study, the aim is to synthesize a porous ceramic based on clay and hydroxyapatite nanoparticles so that the nanoparticles are dispersed inside the ceramic. Also in this study, porosity in sponge-like ceramics is created by using free waste (hair from the hairdresser), the wastewater easily penetrates into the micro-channels and heavy metal ions are adsorbed in the active sites.

2. Experiment

2.1. Material

Natural clay was prepared from Lalejin city, Hamadan province, Iran (The physicochemical properties of natural clay are presented in Table 1). Bovine bones were prepared and cleaned of meat, to remove the adipose tissue, the bones were immersed in boiling water at 120 ℃ for 3 h, the boiling was repeated 4 times, then the bones were crushed using a 5 kg hammer to size of 5 mm. Human hair at 10 mm long was collected from the hairdresser and washed twice with water at 50 ℃ and then dried at room temperature for 2 day. Hydrochloric acid 37%, Nitric acid 65%, sodium hydroxide, $NiN_2O_6.6H_2O$ and, $CoN_2O_6.6H_2O$ were purchased from Sigma-Aldrich company. Two samples of industrial wastewater containing nickel and cobalt ions, respectively, were collected from the zinc ingot factory.

2.2. Preparation of sponge-like nanocomposite ceramics

The crushed bovine bones were placed in a planetary ball mill (Fara Pajouhesh, Isfahan FP2, Iran) at 600 rpm for 2 h. The

Table 1 Physicochemical properties of natural clay.

CEC*(m_{eq} /100 g)	CE**(μS)	pH	Ca^{2+}(m_{eq} /100 g)	Mg^{2+}(m_{eq} /100 g)	Na^{+}(m_{eq} /100 g)	K^{+}(m_{eq} /100 g)
28.36	750	8.3	18.31	9.14	0.62	0.81

* CEC: Cation exchange capacity
** CE: Electrical conductivity

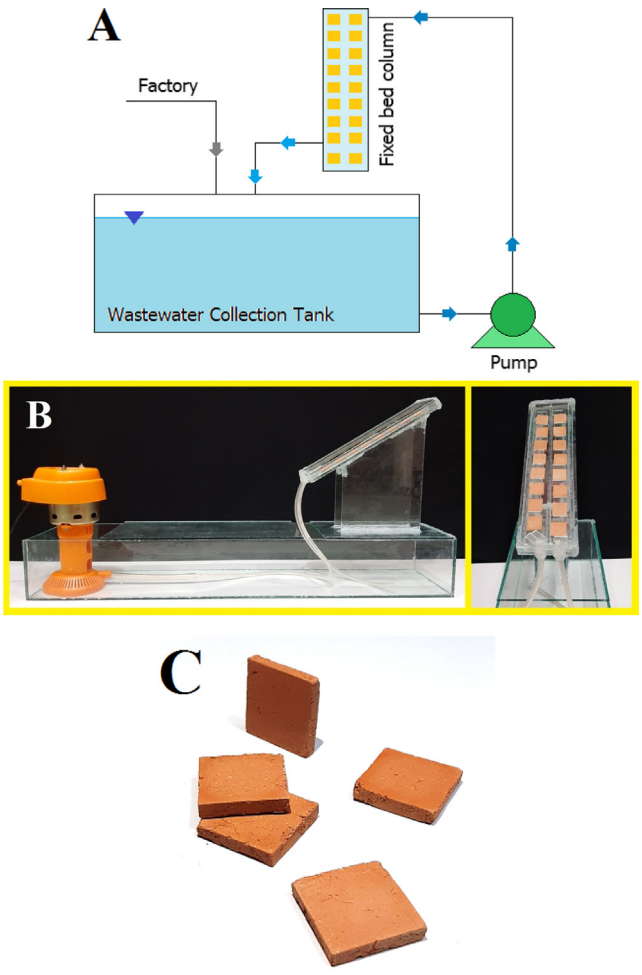

Fig. 1 Schematic of the adsorption process (a), Fixed bed column for installation of nanocomposite ceramics and tank equipped with a pump for Ni(II) wastewater circulation (b), Photographed image of sponge-like nanocomposite ceramics (c).

bovine bone powder (10–120 g), 250 g of natural clay, 50 g of human hair and, 200 g distilled water mixed in a steel container, using a high-powered laboratory mechanical stirrer for 30 min for uniform mixing. The mixture of ceramic compounds was transferred to a mold with dimensions of 20 mm × 20 mm × 4 mm using a Plexiglas stencil (**Fig. S1**). Then composite ceramics dried at room temperature for 4 day (The mass of the ceramics was measured and recorded for 10 days, after 4 days no changes in the mass were observed, so 4 days were chosen to dry the ceramics). Human hair in the ceramic structure prevented the ceramic from cracking and breaking during the initial drying stage. The ceramics were calcined in an electric furnace at 850 ℃ for 12 h. Also, the rate of temperature rise is one of the important parameters in the formation of the uniform structure of nano-hydroxyapatite. Therefore, in this process, the rate of temperature increase was selected based on the results of previous researches of 5 ℃ min^{-1} (Cui et al., 2018; Khadijah et al., 2020). Human hair burns and disappears in the building of ceramic substrates at high temperatures, creating a spongy structure in its void.

2.3. Batch adsorption studies

Adsorption experiments are performed on a fixed bed column with a circulation flow. Fig. 1 **a** shows a schematic of the adsorption process. According to Fig. 1 **b** the Fixed bed column with a square cross section was made of glass with a height of 25 cm and sides with 1 cm × 6 cm. Sponge-like nanocomposite ceramics (Fig. 1 **c**) were installed inside this column. The cooler pump (Model Alborz 220 V, Electrogen Co. Iran) was installed under the column to circulate the fluid. In each batch adsorption process, 10 L of wastewater entered the column. The effective factors in the adsorption process included: pH, adsorbent dose, temperature, initial ion concentration and retention time. The experiments were designed based on central composite design (CCD) in the standard response surface method (RSM). Table 2 shows the ranges as well as the coded and uncoded levels of the variables considered in this study. Design-Expert software suggested an experiments pattern with 50 runs, **Table S1** shows runs and the result of each batch process. In each batch process, the heavy metal ions removal efficiency and adsorption capacity were calculated by Eq. (1) and (2), respectively:

$$R\% = \frac{C_0 - C_t}{C_0} \times 100 \quad (1)$$

$$Q = \frac{(C_0 - C_t)V}{M} \quad (2)$$

where C_0 is Ni(II) or Co(II) initially concentrations $(mg\ L^{-1})$, C_t is Ni(II) or Co(II) concentrations $(mg\ L^{-1})$ at a given time, R% is removal efficiency, V is the volume of wastewater (L),

Table 2 Values of independent variables at different levels of CCD.

Independent variable	Symbol	Levels				
		−2	−1	0	+1	+2
pH	X_1	3	4.5	6	7.5	9
Mass of adsorbent (g)	X_2	4.5	9	13.5	18	22.5
Temperature (℃)	X_3	25	32.5	40	47.5	55
Initial ion concentration (mgL^{-1})	X_4	5	128.75	252.5	376.25	500
Retention time (min)	X_5	10	67.5	125	182.5	240
Response						
Nickel removal efficiency	R_{Ni} (%)					
Cobalt removal efficiency	R_{Co} (%)					

M is mass of adsorbent (g) and Q is a dsorption capacity (mg g^{-1}).

2.4. Measurement and methods

FT-IR spectra (C88731 spectrophotometer, Perkin Elmer Co., Germany) in the range of 400–4000 cm^{-1} was used to identify adsorbent functional groups. The morphology of sponge-like nanocomposite ceramics was investigated using field emission scanning electron microscopes (FE-SEM, TE-SCAN, Czech). The structure of sponge-like ceramic adsorbents was analyzed using X-ray diffraction (Philips PW3040). The pore structure is an important factor in the adsorption of heavy metal ions on the adsorbent, so BET and the pore structure of nanocomposite ceramic were calculated by BET analysis (Costech Sorptometer 1042). The concentration of metal ions was measured using atomic absorption (Varian Atomic Adsorption 240 spectrometer).

2.5. Mechanical strength and chemical resistance tests

Mechanical strength was calculated based on three-point bending tests method, using a manual hydraulic press device (Perkin Elmer Co., Germany). The sponge-like ceramic was placed on two steel rods with a diameter of 3 mm (The distance between the two bars was 10 cm.) and the pressure was applied from above on the center of the sponge-like ceramic at a loading rate of 1 mmmin^{-1}. The pressure that caused the ceramic to break was recorded (Beni and Esmaeili, 2020). To evaluate the chemical resistance, the sponge-like nanocomposite ceramics were placed in an acidic (HNO_3, pH 1) or alkaline (NaOH, pH 13) solution and the weight loss of the ceramic was calculated per hour (Shameli and Ameri, 2017; Torabi and Ameri, 2016) by **Eq. (3)**:

$$\text{Weight loss } (\%) = \frac{W_1 - W_t}{W_1} * 100 \quad (3)$$

where W_1 (g) is mass of sponge-like nanocomposite ceramics after 1 h and W_t (g) is mass of sponge-like nanocomposite ceramics after t hour.

2.6. Development of regression model equation

According to experimental results and its predicted **(Table S1)**, the quadratic model was selected for response, that this model proposed by the software. This model with significant terms was expressed by **Eq. (4)** and **Eq. (5)** for removal of Ni(II) and Co(II), respectively:

$$\begin{aligned} R_{Ni}(\%) = {} & +75.19 + 2.77X_1 + 6.69X_2 + 3.86X_3 - 3.22X_4 \\ & + 20.08X_5 - 4.89X_1^2 - 1.86X_2^2 - 2.63X_3^2 \\ & - 2.86X_4^2 - 7.43X_5^2 \end{aligned} \quad (4)$$

$$\begin{aligned} R_{Co}(\%) = {} & +63.38 + 2.33X_1 + 5.64X_2 + 3.25X_3 - 2.71X_4 \\ & + 16.93X_5 - 4.12X_1^2 - 1.57X_2^2 - 2.22X_3^2 \\ & - 2.41X_4^2 - 6.27X_5^2 \end{aligned} \quad (5)$$

A positive sign against each term of the **Eq. (4)** and **Eq. (5)** indicates a synergistic effect and the negative sign indicates a synergistic effect on the response surface (R).

The actual responses versus predicted responses in **Fig. S2 a** shown approximately a linear relationship with partial variation. The normal plot of residuals in **Fig. S2 b** is similar to a straight line indicating that the errors are evenly distributed and therefore support the least squares fit. According to **Fig. S2 c-d**, the residuals versus the predicted response and the residuals versus the experimental run exhibit the residuals has been distributed above and below the x-axis with unusual structure and no obvious pattern. Also, the R^2 values for model equations were 0.981, the adjusted R^2 and predicted R^2 were 0.968 and 0.931, respectively with difference less than 0.2. The analysis of variance (ANOVA) helps to check the accuracy and validity of the proposed model. According to **Table S2** and **Table S3**, based on ANOVA, the models for R_{Ni} and R_{Co} were highly significant with F-value 76.10 and 76.07, respectively; p-value < 0.0001 also, all of the factors (X_1, X_2, X_3, X_4 and X_5) were significant. Therefore, these models are acceptable for the predicted results and optimization of the factors affecting the removal efficiency of Ni(II) and Co (II).

3. Results

3.1. Mechanical properties

Human hair was added to the clay to create micro-channels (50 g of human hair to 450 g clay). The addition of hair also protected the sponge-like ceramic from disintegrating during the drying phase in the environment. Fig. 2**a** show the mechanical strengths of sintered sponge-like ceramics as functions of bone powder mass. The strength of sponge-like ceramics was based on the breaking stress of ceramics in the range of 1.44 to 3.5 bar. Sponge-like ceramics made of clay without bone powder had the highest mechanical strength because the clay particles were placed uniformly next to each other, but with the addition of bone powder, the clay particles were not uniformly placed next to each other, but nano-hydroxyapatite particles were placed between the clay particles. *Beni* et al. (Beni and Esmaeili, 2019) used nano-rubber in clay ceramic, their results showed a breaking pressure was 1.55–1.90 bar. Therefore, adding 100 g of bone powder to 450 g of clay and 50 g of human hair showed acceptable mechanical strength (Break pressure 2.4 bar).

3.2. Chemical resistance

The stability of sponge-like ceramics in acidic and alkaline solution was investigated. Fig. 2 **b** shows the mass reduction of the ceramic, which was immersed in an acidic solution and a base in two separate experiments and its weight was measured at different times. The synthesized sponge-like nanocomposite ceramics showed 0.5% and 3.73% weight loss after immersion in the NaOH solution (pH 13) and HNO_3 solution (pH 1) respectively, after 24 h. In the concentrated NaOH solution, the mass loss is negligible, but in the acidic solution weak resistance was observed and the sponge-like ceramic was corroded. According to *Mouiya* et al. (Mouiya et al., 2018), the results show that the nano-hydroxyapatite in ceramic tissue dissolves in acidic solution.

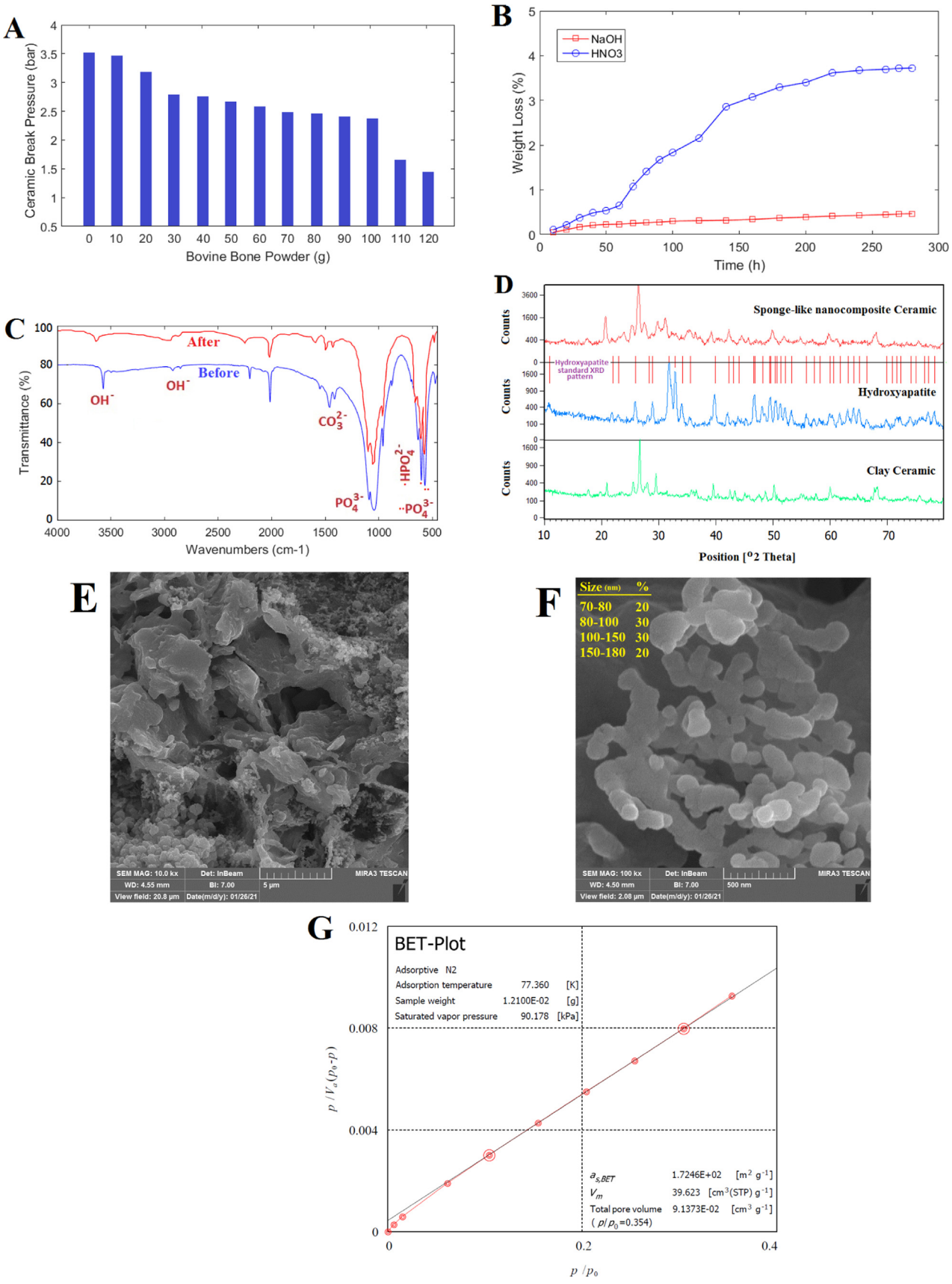

Fig. 2 Effect of bone powder mass (added to 450 g of clay and 50 g of hair) on the mechanical strength of sponge-like nanocomposite ceramics (a), Weight loss of the sintered sponge-like nanocomposite ceramic in nitric acid (pH 1) and sodium hydroxide (pH 13) solutions as a function of time at ambient temperature (b), FT-IR spectra of sponge-like nanocomposite (c), X-ray diffraction profiles of clay ceramic, hydroxyapatite and, sponge-like nanocomposite ceramic (d). The FE-SEM image of sponge-like nanocomposite ceramics (e-f), BET and the pore structure of nanocomposite ceramic (g).

3.3. Characterization of sponge-like nanocomposite ceramics

According to Fig. 2 **c** was presented the FT-IR spectrum of sponge-like nanocomposite ceramic containing hydroxyapatite with a heat treatment of 750 ℃ before adsorption process. The characteristic signals belonging to the hydroxyl (−OH) and phosphate $(PO_4)^{-3}$ functional groups can be identified at 3573 and 1045 cm^{-1}, respectively. XRD pattern of clay ceramic, hydroxyapatite and, sponge-like nanocomposite ceramic was shown in Fig. 2 **d**. It can be seen that the prepared hydroxyapatite belongs to the hexagonal structural type of hydroxyapatite with space group $P6_3/m$. Based on BET analysis (Fig. 2 **g**), the average surface area of the sponge-like nanocomposite ceramic obtained was 172.46 m^2g^{-1} and total pore volume was 913.73 cm^3g^{-1}. In order to study the morphology of hydroxyapatite nanoparticles and porosity of sponge-like nanocomposite ceramics, the FE-SEM micrographs were presented in Fig. 2 **e-f**. Hydroxyapatite nanoparticles were observed in clay ceramics around porous spaces with an average diameter of 100 nm.

3.4. Water permeability in sponge-like nanocomposite ceramic

An innovative method was used to investigate the distilled water permeability inside sponge-like nanocomposite ceramics. According to Fig. 3 **a** in this method a piece of sponge-like ceramic was installed at the bottom of a column 20 cm high and 4 cm in diameter. Fig. 3 **b** shows the relationship between the water level in the column and the average mass flow rate. The results showed that the physical structure of ceramic is very porous, similar to sponge. Water can seep into the sponge-like ceramic and drain from the other surface of the sponge-like ceramic. The sponge-like structure was created due to the use of human hair in the manufacture of nanocomposite ceramics.

3.5. Adsorption test

3.5.1. Effect of solution pH

The pH is an important factor in the adsorption of heavy metal ions on the adsorbent based on clay (Sáez et al., 2020), because pH affects the degree of ionization, the solubility of heavy metal ions changes with pH, also effective in developing the opposite electric charge in the adsorbent surface functional groups (Vahdat et al., 2019). At low pH (pH less than 4), large amounts of H^+ ions surround the adsorbent surface and compete with Ni(II) ions for adsorption on adsorbent active sites (Beni, 2021). Hubadillah et al. (Hubadillah et al., 2020) synthesized a bio-ceramic based on hydroxyapatite using from waste cow bone to textile wastewater treatment; they reported that at a pH 7.3 bio-ceramic surfaces it has a negative charge and is more suitable for absorbing positive ions; while, Googerdchian et al. (Googerdchian et al., 2018) showed that the mechanism of Pb(II) adsorption on nano-hydroxyapatite is dissolution-precipitation and, at low pH 3 the dissolution of hydroxyapatite increases significantly and formed hydroxypyromorphite, $Pb_{10}(PO_4)_6(OH)_2$. Effect of solution pH on the Ni(II) and Co (II) removal efficiency (R %) presented in Fig. 4 **a**, where the mass of clay nanocomposite ceramic, temperature, initial concentration and retention time were fixed at 13.5 g, 40 ℃, 252.5 mgL^{-1}, and 125 min, respectively. The results show that by increasing the pH from 3 to 6, the adsorption efficiency increased, and then, after pH 6, the removal efficiency decreases. Similar to our results, Pb(II), Cr(VI), Ni(II), and Cd(II) from aqueous solution adsorbed at a pH 6 on calcined clay (Zeng et al., 2019), therefore, at high pH, hydroxyl groups have high efficiency (Gu et al., 2020) and also the stability of sponge-like nanocomposite ceramic improves the adsorption process.

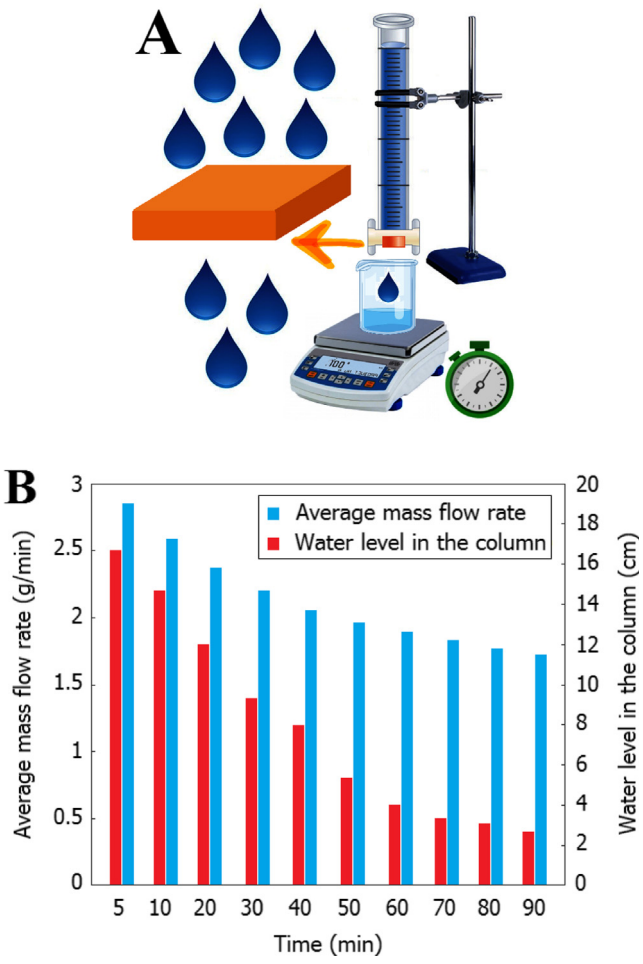

Fig. 3 Schematic of water permeability test in sponge-like nanocomposite ceramic adsorbent (a), The relationship between the water level in the column and the average mass flow rate from the sponge-like nanocomposite ceramic (b).

3.5.2. Effect of temperature

According to the results presented in Fig. 4 **b**, the removal of Ni(II) and Co(II) ions increased with increasing temperature from 25 to 45 ℃. Therefore, at high temperatures, active sites are better available to wastewater by opening the pores of sponge-like nanocomposite ceramics (Saja et al., 2020). *Mnasri-Ghnimi* et al. (Mnasri-Ghnimi and Frini-Srasra, 2019) reported that increasing the removal efficiency at high temperatures suggests that at high temperatures a large number of heavy metal ions obtain sufficient energy to interact with active adsorbent sites (Mnasri-Ghnimi and Frini-Srasra, 2019). Although the physical strength test at different temperatures

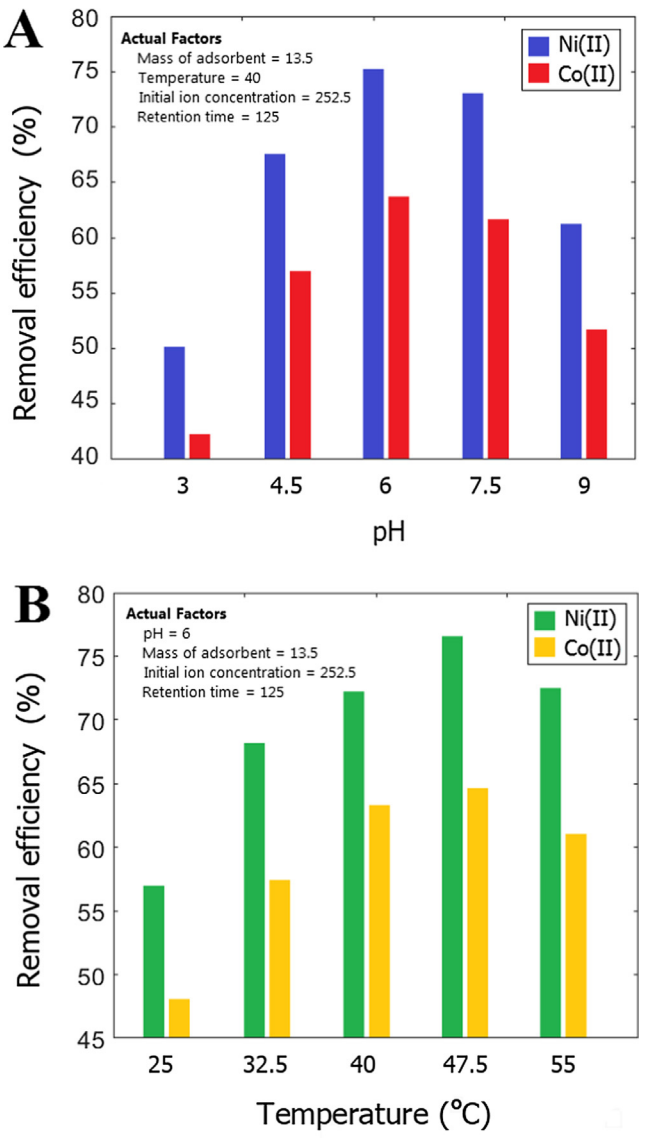

Fig. 4 Effect of pH (a) and temperature (b) on Ni(II) and Co(II) removal efficiency.

showed that the sponge-like nanocomposite ceramic is stable, but the removal efficiency of Ni(II) and Co(II) ions at temperatures above 47 ℃ has decreased, indicating that as the ion is adsorbed, a number of adsorbed ions are separated from the adsorbent surface.

3.5.3. Effect of adsorbent mass and initial concentration

The absorbent dose plays a role in making the process economical (Soliman and Moustafa, 2020). Where dose is the sum of the sponge-like nanocomposite ceramic substrates mass relative to the total volume of the wastewater. As the adsorbent mass increases, the removal efficiency of heavy metal ions increases (Mnasri-Ghnimi and Frini-Srasra, 2019). The presence of more than the optimal amount of adsorbent causes the active sites of adsorbent to remain unoccupied and the adsorption capacity is reduced (Dias Filho and Do Carmo, 2006). According to Fig. 5 **a-b**, in the fixed condition (pH 6, temperature 40 ℃, initial concentration 252.5 mgL^{-1} and retention time 125 min), with increasing the adsorbent mass from 4.5 to 13.5 g, the removal efficiency of Ni(II) and Co (II) ions with a steep slope has increased and then the slope of the removal efficiency is fixed. The adsorption capacity curve shows that by adding more than 9–13.5 g of adsorbent mass, the adsorption capacity is sharply reduced.

The initial concentration is one of the effective parameters in the adsorption process. According to Fig. 5 **c-d**, with increasing the concentration of Ni(II) and Co(II) ions from 5 to 180 mgg^{-1}, the removal efficiency increased; also, with increasing the concentration from 180 to 500 mgg^{-1}, the removal efficiency decreased. Therefore, the removal efficiency of heavy metal ions at any concentration corresponds to active sites that are readily available (Gu et al., 2020). However, increasing the initial concentration of heavy metal ions increases the adsorption capacity. Similar to the results of this study, *Es-sahbany* et al. (Es-Sahbany et al., 2019) reported that natural clay has the ability to adsorb Ni(II) ions at concentrations of 180 to 200 with a removal efficiency of about 75%.

3.5.4. Effect of retention time and kinetic models

To determine the equilibrium adsorption time, the change retention time was in the range of 10 to 240 min and the effective parameters in the adsorption were considered constant (pH 6, temperature 40 ℃, initial concentration 252.5 mgL^{-1} and adsorbent mass 13.5 min).

According to Fig. 6 **a-b**, more than 50% of ions removed at 60 min. As increasing the retention time, the removal efficiency increases and, accordingly, the adsorption capacity also increases (El-Nagar et al., 2020). The Ni(II) and Co(II) removal efficiency during start process to 120 min increased from 5 to 73% and 62%, respectively. The adsorption rate decreased as the adsorption process approached equilibrium (at 120 to 180 min) (Vahdat et al., 2019). Removal efficiency remained constant from 180 to 220 min ; therefore, adsorption entered the equilibrium stage after 180 min (Zhang et al., 2020). *Googerdchian* et al. (Googerdchian et al., 2018) reported a Pb(II) adsorption capacity of 200 mgg^{-1} in the adsorption process using hydroxyapatite nanoparticles at 60 min. This study showed that at a retention time of 60 min with an adsorbent mass of 9 g, the adsorption capacity is about 200 mgg^{-1}, while if the retention time is 240 min, the adsorption capacity will be approximately 300 mgg^{-1}.

The pseudo first-order, second-order and, intraparticle diffusion models were used to fit the kinetic data according to **Eq. (6)**, **(7)** and, **(8)** respectively.

$$\log(q_e - q_t) = \log q_e - (\frac{k_1}{2.303})t \quad (6)$$

$$\frac{1}{q_e - q_t} = \frac{1}{q_e} + k_2 t \quad (7)$$

$$q_e = k_3 t^{0.5} + C \quad (8)$$

where q_e and q_t (mgg^{-1}) are the adsorption capacity at equilibrium and t times (min), respectively. The k_1 in the pseudo first-order model (min^{-1}), k_2 in the second-order model ($mg(gmin)^{-1}$) and, k_3 in the intraparticle diffusion model ($mgg^{-1}min^{-0.5}$) are the rate constants.

The kinetic rate constants obtained from the kinetic models are given in Table 3. The kinetic data of Ni(II) and Co(II) adsorption with nanocomposite ceramic fitted well using

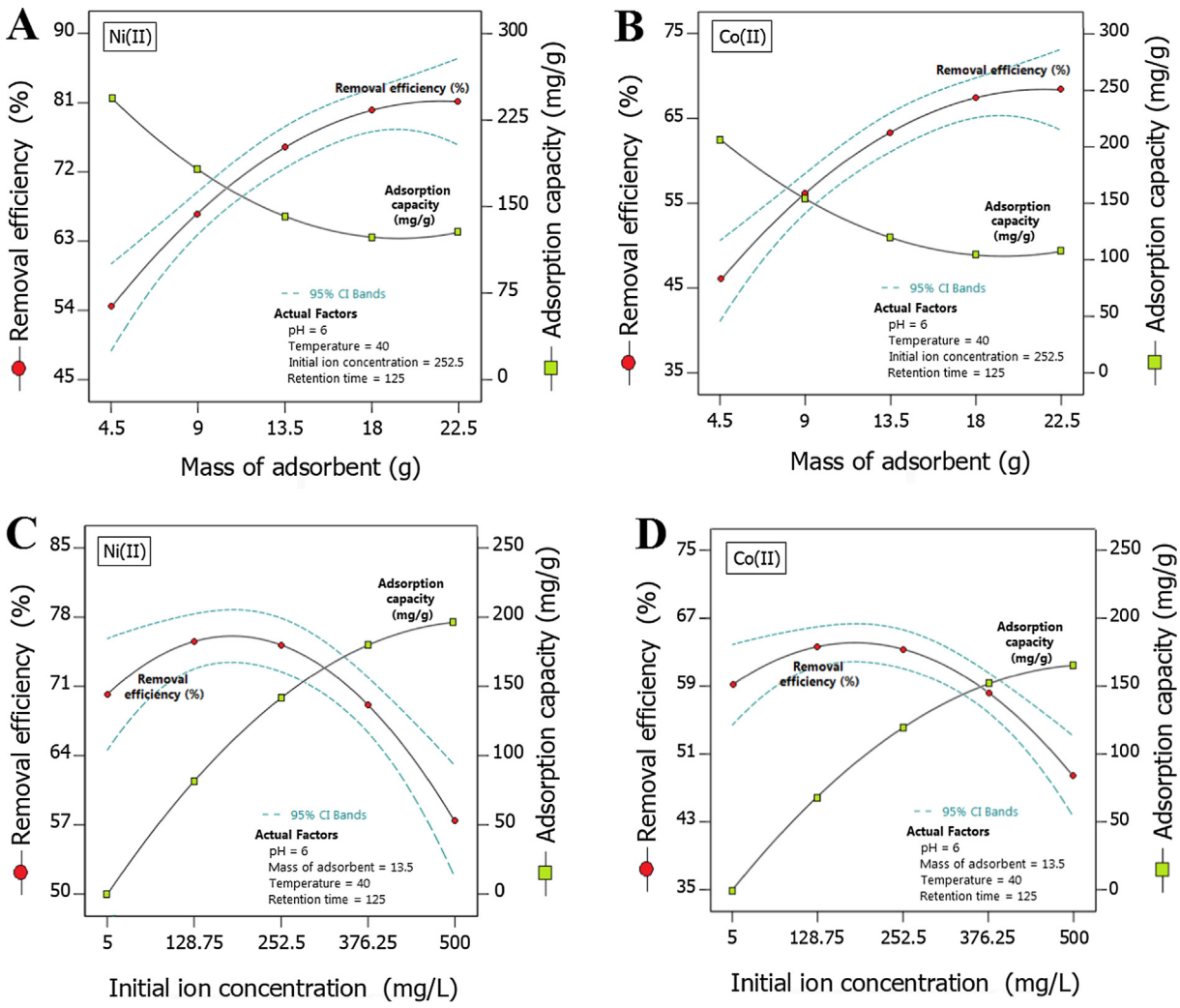

Fig. 5 Effect of adsorbent mass on adsorption capacity of sponge-like nanocomposite ceramic and removal efficiency: Ni(II) wastewater (a) and Co(II) wastewater (b). Effect of initial ion concentration on adsorption capacity of Sponge-like nanocomposite ceramic and removal efficiency: Ni(II) wastewater (c) and Co(II) wastewater (d).

pseudo first-order kinetic model ($R^2 > 0.96$) also, the data of the intraparticle diffusion model with $R^2 > 0.95$ showed that the adsorption proceeds with intraparticle diffusion (diffusion within microchannels) instead of surface adsorption.

4. Process optimization and modeling

In the industrial effluent treatment process, one of the main objectives was to find the optimal adsorption process parameters for economic feasibility with relatively high performance and adsorption capacity of sponge-like nanocomposite ceramics. However, optimizing the process response is difficult because the process is influenced by various factors. Therefore, optimal process performance was applied using Design-Expert software version 11.0.3 (STAT-EASE, Inc., Minneapolis, USA). The software suggested 100 solutions, as shown ramp in Fig. 7, first solution with 0.998 of desirability was selected. Therefore, the optimal conditions were selected as follows: pH 6, mass of sponge-like nanocomposite ceramic 17 g, temperature 45 ℃, initial concentration 233.5 mgL^{-1} and, retention time 180 min.

4.1. Thermodynamic parameters

Gibbs free energy (ΔG), enthalpy (ΔH), and entropy (ΔS) as thermodynamic parameters are calculated from the following equations:

$$\Delta G = -RT \ln K_d \tag{9}$$

$$K_d = \lim_{time \to \infty} \frac{C_{es}}{C_{el}} \tag{10}$$

$$K_d = \frac{C_{es}}{C_{el}} = \frac{C_0 - C_e}{C_0} \tag{11}$$

$$\ln K_d = \frac{\Delta S}{R} - \frac{\Delta H}{RT} \tag{12}$$

where C_{el} and C_{es} (mgL^{-1}) are the values of equilibrium concentration at liquid and solid phase, respectively. T is an absolute temperature (K), R is the gas constant ($8.314 Jmol^{-1}K^{-1}$), and K_d is the distribution coefficient. According to thermodynamic parameter in Table 4, the negative of ΔG indicates the feasibility and spontaneity of Ni(II) and Co(II) adsorption.

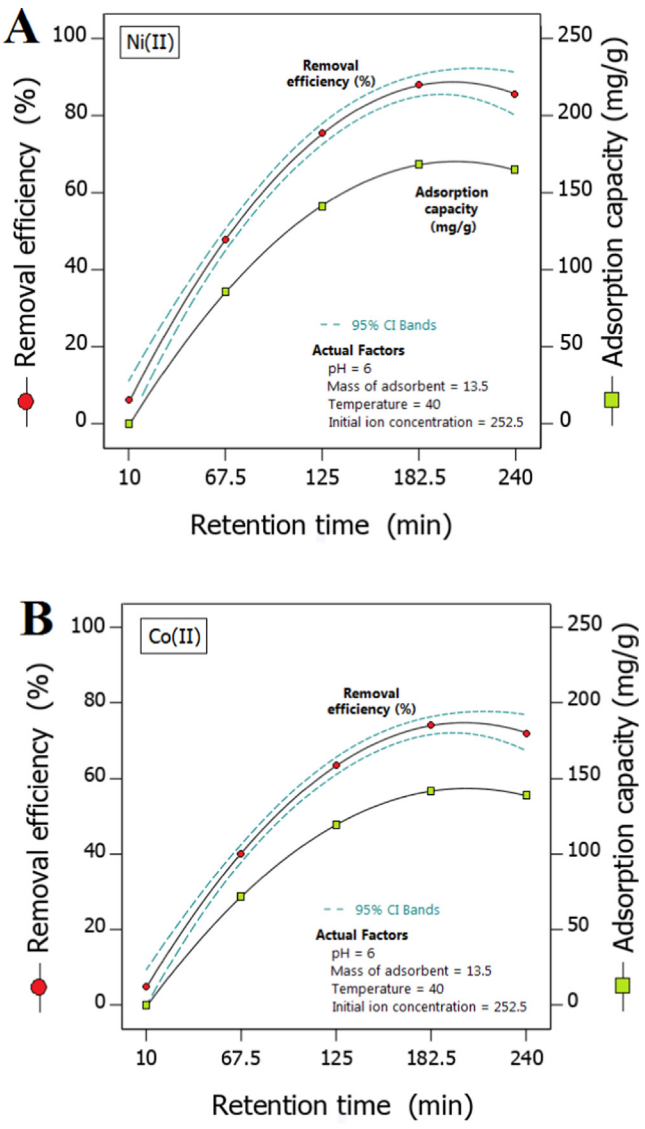

Fig. 6 Effect of retention time on adsorption capacity of sponge-like nanocomposite ceramic and removal efficiency: Ni(II) wastewater (a) and Co(II) wastewater (b).

The positive of ΔH proves the endothermic interaction and, the positive value of ΔS confirms the increased randomness of the solid/liquid interface during the adsorption process.

4.2. Adsorption isotherms

Adsorption isotherm is a valuable curve that describes the phenomenon governing the retention or mobility of a substance from an aqueous medium to a solid phase at constant temperature (Ajiboye et al., 2021). Equilibrium adsorption data were fitted based on different adsorption isotherm models, include: Langmuir, Freundlich and Dubinin-Radushkevich (D-R) isotherm models. In the Langmuir isotherm model assuming that all active sites are the same and adsorption is performed in a single layer in this system (Karimi et al., 2019); In the Friendlich isotherm model, adsorption is considered in several layers of the adsorbent surface. This model can be used for the adsorption process at the heterogeneous surface (Al-Ghouti and Da'ana, 2020) and D-R isotherm can be used to detect the physical adsorption of metal ions from chemical adsorption (Esmaeili and Beni, 2014). Based on the calculations of the parameters and constants of the isotherm models (Table 5), the data fit well with the Langmuir model ($R^2 > 0.98$). Also, the adsorption capacity obtained from the Langmuir model is closer to the actual adsorption capacity of the sponge-like nanocomposite adsorbent than Freundlich isotherm model. According to Table 4 the results of data fitting with the D-R model, the free adsorption energy was calculated to be less than 8kJmol^{-1}, so the adsorption process of Ni(II) and Co (II) on the nanocomposite surface indicate a physical ion exchange.

4.3. Adsorption mechanism

The sponge-like nanocomposite ceramic substrates synthesized in this study were prepared from two main components (natural clay base and hydroxyapatite additive component). Therefore, this soil-bone adsorbent has surface and structural properties of natural clay and hydroxyapatite. So that there are many functional groups in this adsorbent and show complex adsorption mechanisms relative to heavy metal ions (Zhang et al., 2021b). The montmorillonite clays used in this study have a permanent negative charge on the surface that balances the negative charge by exchangeable cations (Tajuddin et al., 2020). Adsorbable exchangeable cations are replaced by Ni(II) and Co(II) heavy metal ions. According to Fig. 2 **c**, which shows the FTIR spectrum before and after the adsorption process, ion exchange between the cation ions of the heavy metals Ni(II) and Co(II) takes place in functional groups such as $(-OH)$ and $(PO_4)^{-3}$ which is represented by hydroxyapatite. Therefore, ion exchange is one of the main mechanisms in this process.

5. Application for the treatment of industrial wastewater

The characteristics of industrial effluent are presented in Table 6 and concentration of other metal ions in wastewater samples are presented in Table 7. It should be noted that due to the low concentration of other heavy metal ions, these ions have no effect on the adsorption process because their concentration is less than 0.5 mgL^{-1}. Due to the process opti-

Table 3 Summary of sorption data evaluated by different kinetic models.

Wastewater sample	q_{max}(mgg^{-1})	Pseudo first – order model			Pseudo second – order model			Intraparticle diffusion model		
		q_e(mgg^{-1})	K_1(min^{-1})	R^2	q_e(mgg^{-1})	K_2(mg g^{-1} min^{-1})	R^2	K_3(mg g^{-1} min$^{-0.5}$)	C	R^2
Ni(II)	129.54	160.92	0.019	0.962	38.91	0.0009	0.659	9.725	5.21	0.957
Co(II)	100.84	133.32	0.018	0.967	89.44	0.0007	0.752	8.507	16.60	0.956

Table 4 Thermodynamic parameters for metal adsorption onto the sponge-like nanocomposite ceramic.

Wastewater sample	K_d			$\Delta H(kJmol^{-1})$	$\Delta S(kJmol^{-1})$	$\Delta G\ (kJmol^{-1})$			R^2
	30 ℃	40 ℃	50 ℃			30 ℃	40 ℃	50 ℃	
Ni(II)	4.61	11.41	11.87	67.514	0.235	−3.85	−6.34	−6.65	0.991
Co(II)	2.26	3.45	3.49	34.16	0.113	−2.05	−3.22	−3.36	0.952

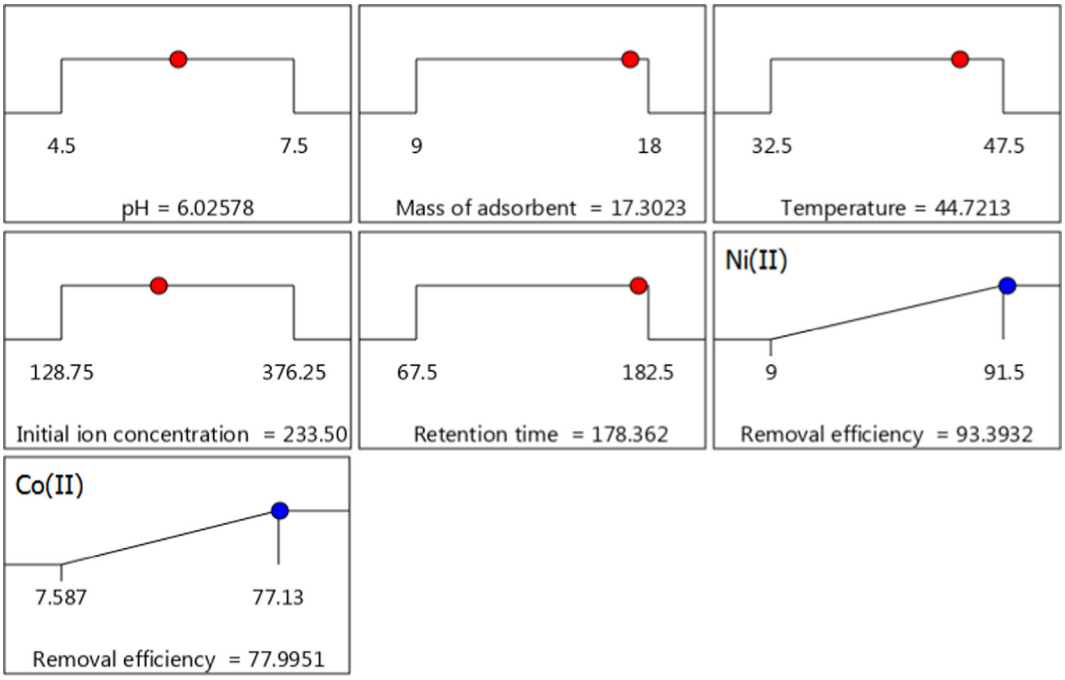

Fig. 7 Desirability ramp for the numerical optimization of affecting factors on the process response.

Table 5 Isotherm parameters for metal adsorption onto the sponge-like nanocomposite ceramic.

Wastewater sample	Langmuir			Freundlich			Dubinin–Radushkevich			
	$q_{max}(mgg^{-1})$	$b(Lmg^{-1})$	R^2	$K_F(mgg^{-1})$	n	R^2	$q_{DR}(mmolg^{-1})$	$\beta_{DR}(mol^2J^{-2})$	$E(kJmol^{-1})$	R^2
Ni(II)	277.78	0.0498	0.998	25.749	1.982	0.918	205.82	0.00002	0.158	0.928
Co(II)	357.14	0.0054	0.983	4.086	1.267	0.937	196.88	0.0001	0.071	0.923

mization in the treatment of synthetic wastewater, this optimized system was used to treat industrial wastewaters. In both effluent samples, the pH was in the range of 6 and there was no need to use acid or alkali to adjust the pH. The results showed that sponge-like nanocomposite ceramics can adsorb heavy metal ions more than 95%. The turbidity did not increase during the process, so sponge-like ceramics have high mechanical strength and the hydroxyapatite particles inside the ceramic are well fixed. Due to the permeability of water in the ceramic sponge-like structure, the fluid flows by gravity, so this process is economically suitable for use in industry. Table 8 offers a comparison between different adsorbents.

Table 6 Analysis of two samples of industrial wastewater containing Ni(II) and Co(II) ions, before and after the adsorption process.

Wastewater sample	Before			After		
	Concentration (mgL^{-1})	Turbidity (NTU)	pH	Concentration (mgL^{-1})	Turbidity (NTU)	pH
Ni(II)	82.45	178	6.31	2.24	165	6.17
Co(II)	43.45	182	6.24	1.55	171	6.21

Table 7 Concentration of other metal ions in wastewater samples.

Metal ions	Concentration (mgL^{-1})
Cu(II)	0.0122
Zn(II)	0.0112
Fe(III)	0.0051
Mg(II)	0.0116

6. Regeneration of sponge-like nanocomposite ceramic substrates

One of the main concerns of using different adsorbents is the regeneration of the adsorbent for reuse and thus reducing the disposal of solid waste. Based on the industrial wastewater treatment, the sponge-like nanocomposite ceramic substrates were regenerated after each cycle of the adsorption process (treatment of 10 L of industrial wastewater) by immersing them in hydrochloric acid 37% for 30 min at room temperature and then rinsing with water (Yadav et al., 2019). Adsorption experiments were repeated for 70 consecutive cycles. According to Fig. 8, the results showed that 60 cycles, the sponge-like nanocomposite ceramic substrates can remove Ni (II) and Co(II) heavy metal ions from industrial wastewater without reducing the removal efficiency.

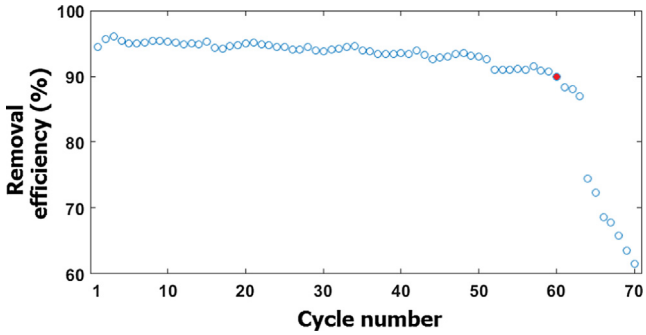

Fig. 8 Heavy metal ion removal efficiency after successive regenerations of the adsorbent.

Table 8 Comparison of heavy metal ion adsorption results using different adsorbents.

Adsorbent	Ions	pH	Adsorbent Dose (mgL^{-1})	Adsorption Capacity (mgg^{-1})	Retention Time (min)	Temperature (℃)	Ref.
Natural clay	Ni (II)	7	63.33	2.4	80	25	(Es-Sahbany et al., 2019)
Natural clay	Cd (II)	5.6	50	1.19	60	Room Temperature	(Es-sahbany et al., 2021a)
Natural clay	Cu (II) Co (II) Ni (II) Pb (II)	8.5 8 8 8.5	84,838,383	6.25 7.01 5.92 6.83	85,848,583	Room Temperature	(Es-sahbany et al., 2021b)
Fe3O4@ coal fly ash porous ceramic	Cu (II)	5.6	–	13.82	120	41.8	(Zhang et al. (2021a)
Calcined clay	Pb (II) Cr (VI) Cd (II)	6	60	32.8 20.3 28.2	200	Room Temperature	(Khalfa et al., 2021)
Waste brick slag	Se (IV)	7	50	58	60	Room Temperature	(Wu et al., 2021)
Plateau laterite ceramic	As (II) Cr (II) Pb (II) Cu (II) Cd (II) Hg (II)	677,899	10,000	2.84 2.38 2.27 2.30 1.99 1.90	960	25	(Zhu et al., 2021)
Sponge-like nanocomposite ceramic	Ni (II) Co (II)	6	17,000	150,110	178	40	In this study

7. Conclusion

The results presented in this study show that clay nanocomposite ceramic with a sponge-like physical structure can be used in industrial applications because it has high removal efficiency and free materials are used in its synthesis. The advantage of this adsorption process at the pH 6 is that the effluent leaves the adsorption stage without the need for any acid-base neutralization process. Based on the findings of this study, different adsorbents can be dispersed at the nanoparticle scale in a substrate such as clay ceramic and provide the necessary space for the effluent to pass through the substrate by creating many microchannels, with this technique, nano-hydroxyapatite adsorbent was synthesized in one step with clay ceramics at 850 ℃. Using human hair, which is a worthless waste, is a good choice to create a microchannel. The sponge-like nanocomposite ceramic with and light weight showed high resistance to mechanical and chemical stresses. The adsorption process using adsorbent substrates is basically slow but the results showed that a large volume of effluent was treated. This process was spontaneous and endothermic, so the adsorption efficiency improved with increasing temperature. The results of adsorbent regeneration showed that sponge-like nanocomposite ceramic substrates can be used for up to 60 consecutive cycles without reducing the removal efficiency of heavy metal ions.

Declaration of Competing Interest

The authors declare that they have no known competing financial interests or personal relationships that could have appeared to influence the work reported in this paper.

References

Ajiboye, T.O., Oyewo, O.A., Onwudiwe, D.C., 2021. Simultaneous removal of organics and heavy metals from industrial wastewater: A review. Chemosphere 262,. https://doi.org/10.1016/j.chemosphere.2020.128379 128379.

Akbarzadeh, M.J., Hashemian, S., Mokhtarian, N., 2020. Study of Pb (II) removal ZIF@NiTiO3nanocomposite from aqueous solutions. J. Environ. Chem. Eng. 8,. https://doi.org/10.1016/j.jece.2020.103703 103703.

Al-Ghouti, M.A., Da'ana, D.A., 2020. Guidelines for the use and interpretation of adsorption isotherm models: A review. J. Hazard. Mater. 393, 122383. https://doi.org/10.1016/j.jhazmat.2020.122383

Beni, A.A., 2021. Design of a solar reactor for the removal of uranium from simulated nuclear wastewater with oil-apatite ELM system. Arab. J. Chem. 14,. https://doi.org/10.1016/j.arabjc.2020.102959 102959.

Beni, A.A., Esmaeili, A., 2020. Environmental Technology & Innovation Biosorption, an efficient method for removing heavy metals from industrial effluents: A Review. Environ. Technol. Innov. 17,. https://doi.org/10.1016/j.eti.2019.100503 100503.

Beni, A.A., Esmaeili, A., 2019. Design and optimization of a new reactor based on biofilm-ceramic for industrial wastewater treatment. Environ. Pollut. 255,. https://doi.org/10.1016/j.envpol.2019.113298 113298.

Cui, H., Shi, Y., Zhou, J., Chu, H., Cang, L., Zhou, D., 2018. Effect of different grain sizes of hydroxyapatite on soil heavy metal bioavailability and microbial community composition. Agric. Ecosyst. Environ. 267, 165–173. https://doi.org/10.1016/j.agee.2018.08.017.

Dias Filho, N.L., Do Carmo, D.R., 2006. Study of an organically modified clay: Selective adsorption of heavy metal ions and voltammetric determination of mercury(II). Talanta 68, 919–927. https://doi.org/10.1016/j.talanta.2005.06.028.

Ebadzadeh, T., Behnamghader, A., Nemati, R., 2011. Preparation of porous hydroxyapatite ceramics containing mullite by reaction sintering of clay, alumina and hydroxyapatite. Ceram. Int. 37, 2887–2889. https://doi.org/10.1016/j.ceramint.2011.02.020.

El-Nagar, D.A., Massoud, S.A., Ismail, S.H., 2020. Removal of some heavy metals and fungicides from aqueous solutions using nano-hydroxyapatite, nano-bentonite and nanocomposite. Arab. J. Chem. 13, 7695–7706. https://doi.org/10.1016/j.arabjc.2020.09.005.

Ersan, M., Asli, U., Acıkel, U., Sarioglu, M., 2015. Synthesis of hydroxyapatite / clay and hydroxyapatite / pumice composites for tetracycline. Process Saf. Environ. Prot. 96, 22–32. https://doi.org/10.1016/j.psep.2015.04.001.

Es-Sahbany, H., Berradi, M., Nkhili, S., Hsissou, R., Allaoui, M., Loutfi, M., Bassir, D., Belfaquir, M., El Youbi, M.S., 2019. Removal of heavy metals (nickel) contained in wastewater-models by the adsorption technique on natural clay. Mater. Today Proc. 13, 866–875. https://doi.org/10.1016/j.matpr.2019.04.050.

Es-sahbany, H., El Hachimi, M.L., Hsissou, R., Belfaquir, M., Es-sahbany, K., Nkhili, S., Loutfi, M., Elyoubi, M.S., 2021a. Adsorption of heavy metal (Cadmium) in synthetic wastewater by the natural clay as a potential adsorbent (Tangier-Tetouan-Al Hoceima – Morocco region). Mater. Today Proc. 45, 7299–7305. https://doi.org/10.1016/j.matpr.2020.12.1102.

Es-sahbany, H., Hsissou, R., El Hachimi, M.L., Allaoui, M., Nkhili, S., Elyoubi, M.S., 2021b. Investigation of the adsorption of heavy metals (Cu Co, Ni and Pb) in treatment synthetic wastewater using natural clay as a potential adsorbent (Sale-Morocco). Mater. Today Proc. 45, 7290–7298. https://doi.org/10.1016/j.matpr.2020.12.1100.

Esmaeili, A., Beni, A.A., 2014. A novel fixed-bed reactor design incorporating an electrospun PVA/chitosan nanofiber membrane. J. Hazard. Mater. 280, 788–796. https://doi.org/10.1016/j.jhazmat.2014.08.048.

Faksawat, K., Limsuwan, P., Naemchanthara, K., 2021. Applied Clay Science 3D printing technique of specific bone shape based on raw clay using hydroxyapatite as an additive material. Appl. Clay Sci. 214,. https://doi.org/10.1016/j.clay.2021.106269 106269.

Googerdchian, F., Moheb, A., Emadi, R., Asgari, M., 2018. Optimization of Pb(II) ions adsorption on nanohydroxyapatite adsorbents by applying Taguchi method. J. Hazardous Mater. Elsevier B.V. https://doi.org/10.1016/j.jhazmat.2018.01.056.

Gu, M., Hao, L., Wang, Y., Li, X., Chen, Y., Li, W., Jiang, L., 2020. The selective heavy metal ions adsorption of zinc oxide nanoparticles from dental wastewater. Chem. Phys. 534,. https://doi.org/10.1016/j.chemphys.2020.110750 110750.

Guo, H., Jiang, C., Xu, Z., Luo, P., Fu, Z., Zhang, J., 2019. Synthesis of bitter gourd-shaped nanoscaled hydroxyapatite and its adsorption property for heavy metal ions. Mater. Lett. 241, 176–179. https://doi.org/10.1016/j.matlet.2019.01.028.

Hamad, A.A., Hassouna, M.S., Shalaby, T.I., Elkady, M.F., Abd Elkawi, M.A., Hamad, H.A., 2020. Electrospun cellulose acetate nanofiber incorporated with hydroxyapatite for removal of heavy metals. Int. J. Biol. Macromol. 151, 1299–1313. https://doi.org/10.1016/j.ijbiomac.2019.10.176.

Hernández-Cocoletzi, H., Salinas, R.A., Águila-Almanza, E., Rubio-Rosas, E., Chai, W.S., Chew, K.W., Mariscal-Hernández, C., Show, P.L., 2020. Natural hydroxyapatite from fishbone waste for the rapid adsorption of heavy metals of aqueous effluent. Environ. Technol. Innov. 20,. https://doi.org/10.1016/j.eti.2020.101109 101109.

Hubadillah, S.K., Othman, M.H.D., Tai, Z.S., Jamalludin, M.R., Yusuf, N.K., Ahmad, A., Rahman, M.A., Jaafar, J., Kadir, S.H.S.A., Harun, Z., 2020. Novel hydroxyapatite-based bio-ceramic hollow fiber membrane derived from waste cow bone for textile

wastewater treatment. Chem. Eng. J. 379,. https://doi.org/10.1016/j.cej.2019.122396 122396.

Karimi, S., Tavakkoli Yaraki, M., Karri, R.R., 2019. A comprehensive review of the adsorption mechanisms and factors influencing the adsorption process from the perspective of bioethanol dehydration. Renew. Sustain. Energy Rev. 107, 535–553. https://doi.org/10.1016/j.rser.2019.03.025.

Khadijah, S., Ha, M., Othman, D., Sheng, Z., Riduan, M., Kamilah, N., Ahmad, A., Rahman, M.A., Jaafar, J., Hamimah, S., Abdul, S., Harun, Z., 2020. Novel hydroxyapatite-based bio-ceramic hollow fi ber membrane derived from waste cow bone for textile wastewater treatment 379. https://doi.org/10.1016/j.cej.2019.122396

Khalfa, L., Sdiri, A., Bagane, M., Cervera, M.L., 2021. A calcined clay fixed bed adsorption studies for the removal of heavy metals from aqueous solutions. J. Clean. Prod. 278,. https://doi.org/10.1016/j.jclepro.2020.123935 123935.

Kundu, K., Afshar, A., Katti, D.R., Edirisinghe, M., Katti, K.S., 2021. Composite nanoclay-hydroxyapatite-polymer fiber scaffolds for bone tissue engineering manufactured using pressurized gyration. Compos. Sci. Technol. 202,. https://doi.org/10.1016/j.compscitech.2020.108598 108598.

Liu, Xiaolu, Pang, H., Liu, Xuewei, Li, Q., Zhang, N., Mao, L., Qiu, M., Hu, B., Yang, H., Wang, X., Liu, Xiaolu, Pang, H., Liu, Xuewei, Li, Q., Zhang, N., Mao, L., Qiu, M., Hu, B., Yang, H., Wang, X., 2021. Orderly Porous Covalent Organic Frameworks-based Materials: Superior Adsorbents for Pollutants Removal from Aqueous Solutions Orderly Porous Covalent Organic Frameworks-based Materials: Superior Adsorbents for Pollutants Removal from Aqueous Solutions. Innov. 2,. https://doi.org/10.1016/j.xinn.2021.100076 100076.

Mnasri-Ghnimi, S., Frini-Srasra, N., 2019. Removal of heavy metals from aqueous solutions by adsorption using single and mixed pillared clays. Appl. Clay Sci. 179,. https://doi.org/10.1016/j.clay.2019.105151 105151.

Mouiya, M., Abourriche, A., Bouazizi, A., Benhammou, A., El Hafiane, Y., Abouliatim, Y., Nibou, L., Oumam, M., Ouammou, M., Smith, A., Hannache, H., 2018. Flat ceramic microfiltration membrane based on natural clay and Moroccan phosphate for desalination and industrial wastewater treatment. Desalination 427, 42–50. https://doi.org/10.1016/j.desal.2017.11.005.

Mouiya, M., Bouazizi, A., Abourriche, A., Benhammou, A., El Hafiane, Y., Ouammou, M., Abouliatim, Y., Younssi, S.A., Smith, A., Hannache, H., 2019. Fabrication and characterization of a ceramic membrane from clay and banana peel powder: Application to industrial wastewater treatment. Mater. Chem. Phys. 227, 291–301. https://doi.org/10.1016/j.matchemphys.2019.02.011.

Padilla-Ortega, E., Leyva-Ramos, R., Flores-Cano, J.V., 2013. Binary adsorption of heavy metals from aqueous solution onto natural clays. Chem. Eng. J. 225, 535–546. https://doi.org/10.1016/j.cej.2013.04.011.

Roychoudhury, P., Majumdar, S., Sarkar, S., Kundu, B., 2019. Performance investigation of Pb (II) removal by synthesized hydroxyapatite based ceramic ultra fi ltration membrane: Bench scale study. Chem. Eng. J. 355, 510–519. https://doi.org/10.1016/j.cej.2018.07.155.

Sáez, P., Dinu, I.A., Rodríguez, A., Gómez, J.M., Lazar, M.M., Rossini, D., Dinu, M.V., 2020. Composite cryo-beads of chitosan reinforced with natural zeolites with remarkable elasticity and switching on/off selectivity for heavy metal ions. Int. J. Biol. Macromol. 164, 2432–2449. https://doi.org/10.1016/j.ijbiomac.2020.08.009.

Saja, S., Bouazizi, A., Achiou, B., Ouaddari, H., Karim, A., Ouammou, M., Aaddane, A., Bennazha, J., Alami Younssi, S., 2020. Fabrication of low-cost ceramic ultrafiltration membrane made from bentonite clay and its application for soluble dyes removal. J. Eur. Ceram. Soc. 40, 2453–2462. https://doi.org/10.1016/j.jeurceramsoc.2020.01.057.

Shameli, A., Ameri, E., 2017. Synthesis of cross-linked PVA membranes embedded with multi-wall carbon nanotubes and their application to esterification of acetic acid with methanol. Chem. Eng. J. 309, 381–396. https://doi.org/10.1016/j.cej.2016.10.039.

Shen, Q., Luo, L., Bian, L., Liu, Y., Yuan, B., Liu, C., Pan, X., Jiang, F., 2016. Lead cations immobilization by hydroxyapatite with cotton-like morphology. J. Alloys Compd. 673, 175–181. https://doi.org/10.1016/j.jallcom.2016.02.204.

Soliman, N.K., Moustafa, A.F., 2020. Industrial solid waste for heavy metals adsorption features and challenges; a review. J. Mater. Res. Technol. 9, 10235–10253. https://doi.org/10.1016/j.jmrt.2020.07.045.

Tajuddin, M.F., Al-Gheethi, A., Mohamed, R., Noman, E., Talip, B. A., Bakar, A., 2020. Optimizing of heavy metals removal from car wash wastewater by chitosan-ceramic beads using response surface methodology. Mater. Today Proc. 31, 43–47. https://doi.org/10.1016/j.matpr.2020.01.085.

Torabi, B., Ameri, E., 2016. Methyl acetate production by coupled esterification-reaction process using synthesized cross-linked PVA/silica nanocomposite membranes. Chem. Eng. J. 288, 461–472. https://doi.org/10.1016/j.cej.2015.12.011.

Vahdat, A., Ghasemi, B., Yousefpour, M., 2019. Synthesis of hydroxyapatite and hydroxyapatite/Fe3O4 nanocomposite for removal of heavy metals. Environ. Nanotechnol. Monit. Manag. 12,. https://doi.org/10.1016/j.enmm.2019.100233 100233.

Wu, J., Huang, X., Chen, H., Gou, M., Zhang, T., 2021. Fabrication of Cu-Al2O3/ceramic particles by using brick particles as supports for highly-efficient selenium adsorption. J. Environ. Chem. Eng. 9,. https://doi.org/10.1016/j.jece.2020.105008 105008.

Yadav, V.B., Gadi, R., Kalra, S., 2019. Clay based nanocomposites for removal of heavy metals from water: A review. J. Environ. Manage. 232, 803–817. https://doi.org/10.1016/j.jenvman.2018.11.120.

Yu, F., Bai, X., Liang, M., Ma, J., 2021. Recent progress on metal-organic framework-derived porous carbon and its composite for pollutant adsorption from liquid phase. Chem. Eng. J. 405,. https://doi.org/10.1016/j.cej.2020.126960 126960.

Zeng, R., Tang, W., Ding, C., Yang, L., Gong, D., Kang, Z., He, Z., Wu, Y., 2019. Preparation of anionic-cationic co-substituted hydroxyapatite for heavy metal removal: Performance and mechanisms. J. Solid State Chem. 280,. https://doi.org/10.1016/j.jssc.2019.120960 120960.

Zhang, C.J., Hu, M., Ke, Q.F., Guo, C.X., Guo, Y.J., Guo, Y.P., 2020. Nacre-inspired hydroxyapatite/chitosan layered composites effectively remove lead ions in continuous-flow wastewater. J. Hazard. Mater. 386,. https://doi.org/10.1016/j.jhazmat.2019.121999 121999.

Zhang, J., Yan, M., Sun, G., Liu, K., 2021a. An environment-friendly Fe3O4@CFAS porous ceramic: Adsorption of Cu(II) ions and process optimisation using response surface methodology. Ceram. Int. 47, 8256–8264. https://doi.org/10.1016/j.ceramint.2020.11.185.

Zhang, T., Wang, W., Zhao, Y., Bai, H., Wen, T., Kang, S., Song, G., Song, S., Komarneni, S., 2021b. Removal of heavy metals and dyes by clay-based adsorbents: From natural clays to 1D and 2D nanocomposites. Chem. Eng. J. 420,. https://doi.org/10.1016/j.cej.2020.127574 127574.

Zhu, D., He, Y., Zhang, B., Zhang, N., Lei, Z., Zhang, Z., Chen, G., Shimizu, K., 2021. Simultaneous removal of multiple heavy metals from wastewater by novel plateau laterite ceramic in batch and fixed-bed studies. J. Environ. Chem. Eng. 9, 1–9. https://doi.org/10.1016/j.jece.2021.105792.

Zou, X., Zhao, Y., Zhang, Z., 2019. Preparation of hydroxyapatite nanostructures with different morphologies and adsorption behavior on seven heavy metals ions. J. Contam. Hydrol. 226,. https://doi.org/10.1016/j.jconhyd.2019.103538 103538.